SERBIAN JOURNAL OF ELECTRICAL ENGINEERING
Vol. 2, No. 1, May 2005, 63 - 76

The Influence of Plastic Deformation and Chemical Environment on the Resistivity of Al-Alloy Overhead Lines

D. Nowak-Woźny[1], W. Mielcarek[2], K. Prociów[2], L. Woźny[3], J.B. Gajewski[1*]

Abstract: The electrical resistivity and intensity of X-ray diffraction reflexes were determined for overhead line wires deformed plastically and immersed at different solutions. Immersing (chemical ageing) was performed by plastic deformation along the wire axis. During chemical ageing the samples were exposed to the action of the Cl^-, SO_4^{2-}, and SO_3^{2-} ions. Resistivity was measured at room temperature and at liquid nitrogen temperature. After the X-ray and resistivity measurement data were compared, it was found that three processes could take place: the flow of ions through the boundary between a sample and environment; the mechanical relaxation of vacancies near a line of dislocations, and the ordering of microstructure. These effects can lead to the anisotropy of resistivity.

Keywords: Overhead lines; Al–alloy; resistivity; Microstructure; Ageing; X–ray diffraction

1 Introduction

An Al–alloy is used for electric current path in overhead lines. They are exposed to temperature shocks, environment hazards and mechanical stresses [1]. For the self-supporting overhead lines the tensile strength is of prime importance. This work was intended to determine the correlation between environmental hazards, mechanical stresses, wire resistivity and material structure.

An important way for investigating the lattice defects and microstructures is the resistivity measurement. This method is specifically sensitive when the

[1]Department of Electrostatics and Electrothermal Engineering, Institute of Heat Engineering and Fluid Mechanics, Wrocław University of Technology, 50-372 Wrocław, Wybrzeże Wyspiańskiego 27, Poland
[2] Institute of Electrotechnics, M. Skłodowskiej-Curie 55/61, 50- 369 Wrocław, Poland
[3] Institute of Electrical Engineering and Electrotechnology, Wrocław University of Technology, 50-372 Wrocław, Wybrzeże S. Wyspiańs-kiego 27, Poland
[*]Corresponding author. Tel.: +48 71 320 32 01, fax: +48 71 328 38 18; e-mail addresses: gajewski@itcmp.pwr.wroc.pl or juliusz.b.gajewski@pwr.wroc.pl.

resistivity is measured at low temperatures. For the purpose of the work presented the low-temperature (liquid nitrogen) measurements of the resistivity were performed along with those at room temperature for samples aged in different manners. It is expected that the research results will lead to an overhead lines diagnostic method to be used in near future.

After an analysis had been made of widely known theoretical and experimental results obtained by different authors [2,3] it was found that the resistivity of annealed cubic metal is not always isotropic. There is clear evidence that the resistivity of deformed metals is sometimes an isotropic. During the working of polycrystalline aggregates the development of a preferred orientation led to a change in the resistivity [2,3]. It is well known [2] that the longitudinal resistivity may be greater, equal to or smaller than the transverse resistivity. The resistivity differences result from the nonuniformity of dislocations, as does the scattering anisotropy. The plastic deformation causes the movement of dislocations and the creation of new dislocations on a large scale.

The resistivity is sensitive to microstructure changes thus one can therefore study the properties of a given microstructure.

2 Experimental Procedure

The plastic deformation was carried out at room temperature (RT) using an INSTRON 6025 machine at a strain rate of 0.85×10^{-5} m/s. Fig. 1 shows the stress–strain curve. The points shown in the plot represent the degree of plastic deformation of the samples tested. Mechanical deformation was realized by the longitudinal plastic extension of a wire, [4-6]. The environmental hazards were simulated by immersing Al–alloy samples put into aggressive environments of Cl^-, SO_4^{2-}, SO_3^{2} ions.

There were used samples of wires with diameters equal to 2.09–2.10 mm. The commercial alloy wires whose composition was not known and they were made in accordance with the Polish standard for overhead wires PN-74/E-90211.composition was in agreement with PN-74/E-90211.

The samples were prepared from the overhead lines that were not being used and went up and cut off pieces. The samples were immersed and deformed at room temperature (about 20°C). Before the chemical ageing in solutions, the samples were deformed plastically. The samples were immersed (at room temperature) in the water solutions of Nail (3%), Na_2SO_4 (3%), Na_2SO_3 (3%) NaCl (3%)–Na_2SO_4 (3%) and NaCl (3%)–Na_2SO_3 (3%) for 300 days.

The resistivity of each sample was measured before and after deformation at both room and liquid nitrogen temperatures using a bridge P 56/2 and I = 10A, f = 50Hz. The resistivity measurement system is shown in Fig. 2. While the

samples were immersed in the solutions the electrical properties of the samples were inspected at different time intervals.

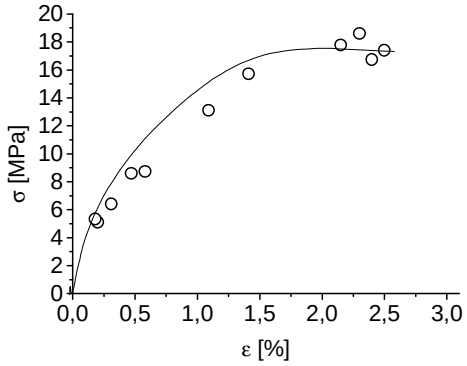

Fig. 1 – *The sample's relative elongation as a function of the tensile stresses applied.*

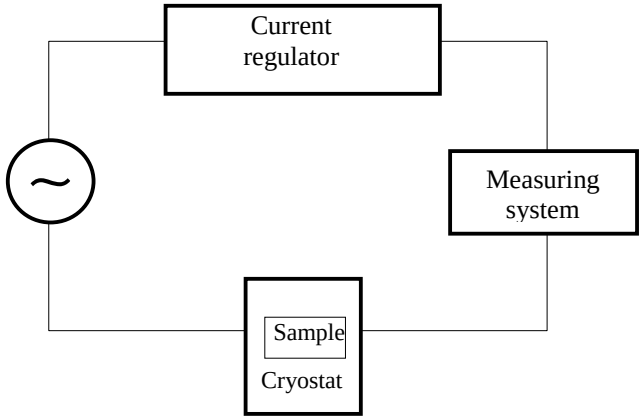

Fig. 2 – *Schematic of the resistivity measuring system.*

The X-ray measurements were carried out on the deformed and chemically aged samples. The samples prepared for the X-ray measurements were the middle sections of the samples; they were arranged in the sets of 5 resin-sealed pieces and positioned parallel to each other. The schematic view of a sample preparation is shown in Fig. 3. To achieve the proper intensities of X-ray reflexes, the samples were polished to a half of their initial width along the wire axis and then smoothed. The X-ray measurements were made using an X-ray difractometer DRON 2 with Co radiation filtered Fe within the angle range

$10 < 2\Theta < 100$ in the Bragg-Brentano standard set [7]. The Al-alloy texture was determined for the following reflections: (111), (002), (022) and (113) in the standard set and for (111), (002) and (022) using a texture attachment. The intensity of reflections was calculated using the X-Rayan program.

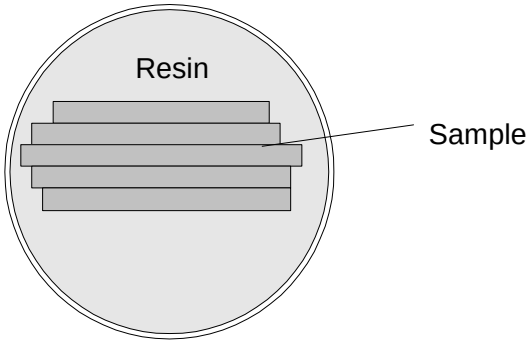

Fig. 3 – *Schematic view of the sample preparation for the X-ray measurements.*

3 Results and Discussion

3.1 Resistivity test

The relative time variations of the sample resistivity were examined that were brought about by the plastic deformation. In general, the changes in relative resistivity and the degree of plastic deformation can be defined as:

$$\rho_T^{rel}(\varepsilon, t) = \frac{\rho_T(\varepsilon, t) - \rho_T(\varepsilon, t=0)}{\rho_T(\varepsilon, t=0)}, \tag{1}$$

where: $\varepsilon = \Delta l / l_0 \, [\%]$, $\rho_T(\varepsilon, t)$ is the resistivity as measured at the temperature T.

The Al wire resistivity that was measured under the aggressive environment action is shown in Figs. 4, 5, 6, 7 and 8. It is important that the resistivity was determined on the assumption that the cross-sectional area of a given wire was always constant.

For times of aging below 40 days and for room temperature (RT), the rate of the changes of $\rho_{RT}^{rel}(\varepsilon, t)$ for nondeformed samples was much higher than for the deformed samples. In the case of the samples deformed and immersed in the solutions of Na_2SO_4 and NaCl–Na_2SO_4, the initial increase in $\rho_{RT}^{rel}(\varepsilon, t)$ within about 20 days was observed. The direction of the $\rho_{RT}^{rel}(\varepsilon, t)$ variations with time

for longer ageing times than 40 days differed qualitatively and quantitatively depending on ageing conditions. In some cases $\rho_{RT}^{rel}(\varepsilon, t)$ increased while in other cases it decreased.

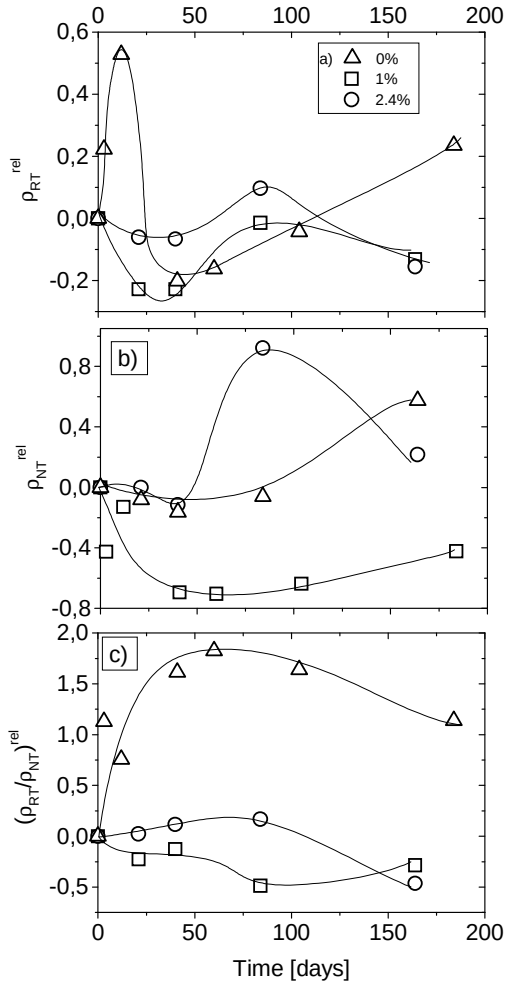

Fig. 4 – *Time variations of:*

a) the resistivity $\rho_{RT}^{rel}(\varepsilon, t)$ *, b) the resistivity* $\rho_{NT}^{rel}(\varepsilon, t)$ *, and*

c) the relative resistivity ratio $(\rho_{RT}/\rho_{NT})^{\mathrm{rel}}(\varepsilon, t)$ *for the samples chemically aged in the water solution of NaCl–*Na_2SO_4 *for the different degree of the plastic deformation.*

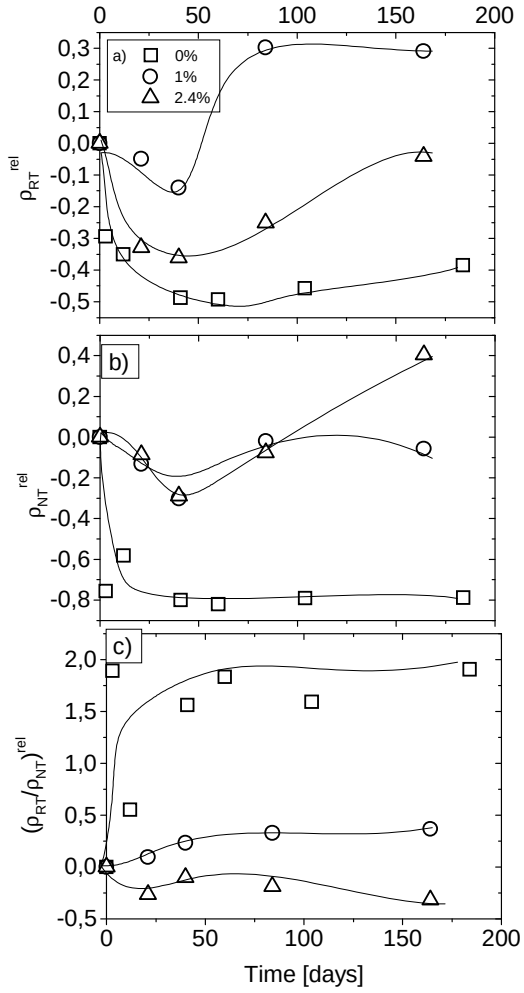

Fig. 5 – *Time variations of:*
a) the resistivity $\rho_{RT}^{rel}(\varepsilon,t)$ *, b) the resistivity* $\rho_{NT}^{rel}(\varepsilon,t)$ *, and*
c) the relative resistivity ratio $(\rho_{RT}/\rho_{NT})^{\mathrm{rel}}(\varepsilon,t)$ *for the samples chemically aged in the water solution of NaCl- Na2SO3 for the different degree of the plastic deformation.*

The plastic deformation also influenced the intensity of the $\rho_{NT}^{rel}(\varepsilon,t)$ changes as measured at the temperature of liquid nitrogen (NT). At the beginning, that is up to 40 days, the $\rho_{NT}^{rel}(\varepsilon,t)$ changes in the nondeformed samples were much higher than in the deformed ones. After 40–60 days of

ageing and for the plastic deformation lower than 2%, the changes in $\rho_{NT}^{rel}(\varepsilon,t)$ differed in character from the changes in $\rho_{NT}^{rel}(\varepsilon,t)$ for the nondeformed material. When the degree of the plastic deformation was higher than 2%, then the $\rho_{NT}^{rel}(\varepsilon,t)$ changes were only quantitative, i.e. the magnitude of the $\rho_{NT}^{rel}(\varepsilon,t)$ changes of the deformed samples for the first 40–60 days was less intensive than that observed in the nondeformed ones.

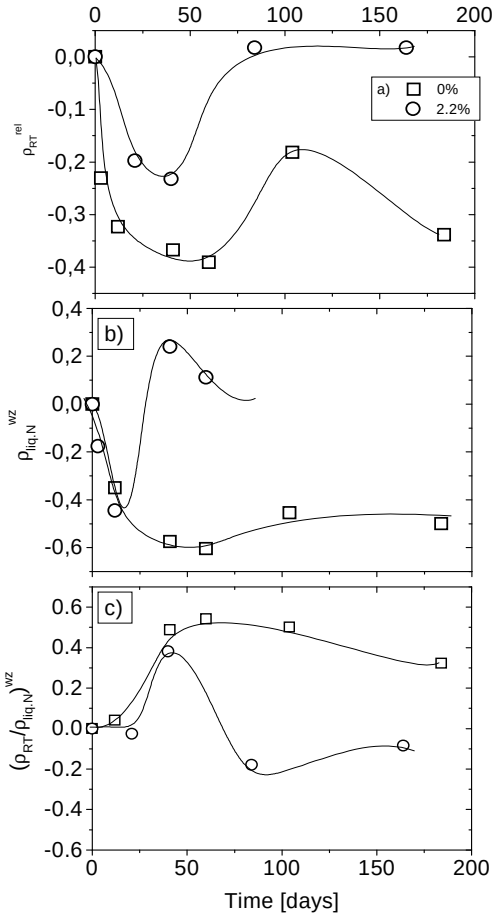

Fig. 6 – *Time variations of:*
a) the resistivity $\rho_{RT}^{rel}(\varepsilon,t)$, *b) the resistivity* $\rho_{NT}^{rel}(\varepsilon,t)$, *and*
c) the relative resistivity ratio $(\rho_{RT}/\rho_{NT})^{\mathrm{rel}}(\varepsilon,t)$ *for the samples chemically aged in the water solution of* Na_2SO_3 *for the different degree of the plastic deformation.*

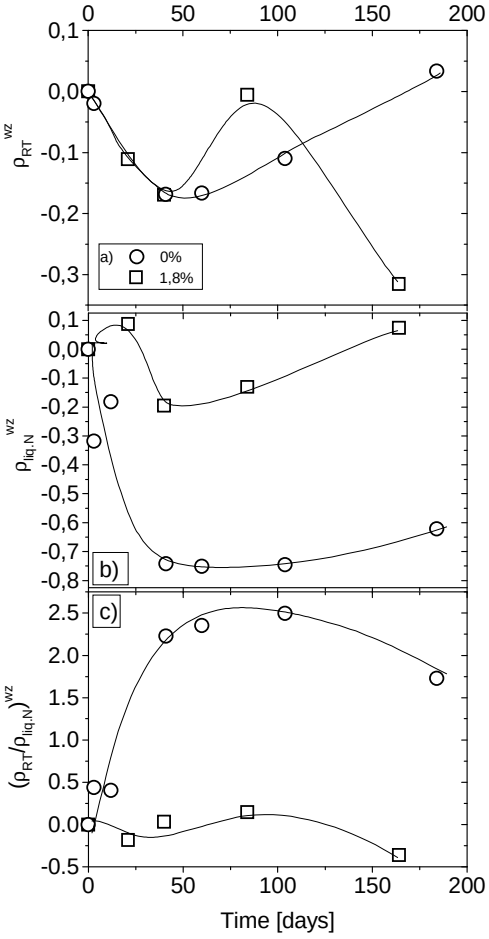

Fig. 7 – *Time variations of:*
a) the resistivity $\rho_{RT}^{rel}(\varepsilon, t)$, *b) the resistivity* $\rho_{NT}^{rel}(\varepsilon, t)$, *and*
c) the relative resistivity ratio $(\rho_{RT}/\rho_{NT})^{\mathrm{rel}}(\varepsilon, t)$ *for the samples chemically aged in the water solution of* Na_2SO_4 *for the different degree of the plastic deformation.*

In Figs. 4–8 one can see that the initial plastic deformation also caused the changes in the relative ratio $(\rho_{RT}/\rho_{NT})^{\mathrm{rel}}(\varepsilon, t)$ that can be expressed in the following form:

$$(\rho_{RT}/\rho_{NT})^{\mathrm{rel}}(\varepsilon,t)=\frac{\dfrac{\rho_{RT}(\varepsilon,t)}{\rho_{NT}(\varepsilon,t)}-\dfrac{\rho_{RT}(\varepsilon,t=0)}{\rho_{NT}(\varepsilon,t=0)}}{\dfrac{\rho_{RT}(\varepsilon,t=0)}{\rho_{NT}(\varepsilon,t=0)}}. \qquad (2)$$

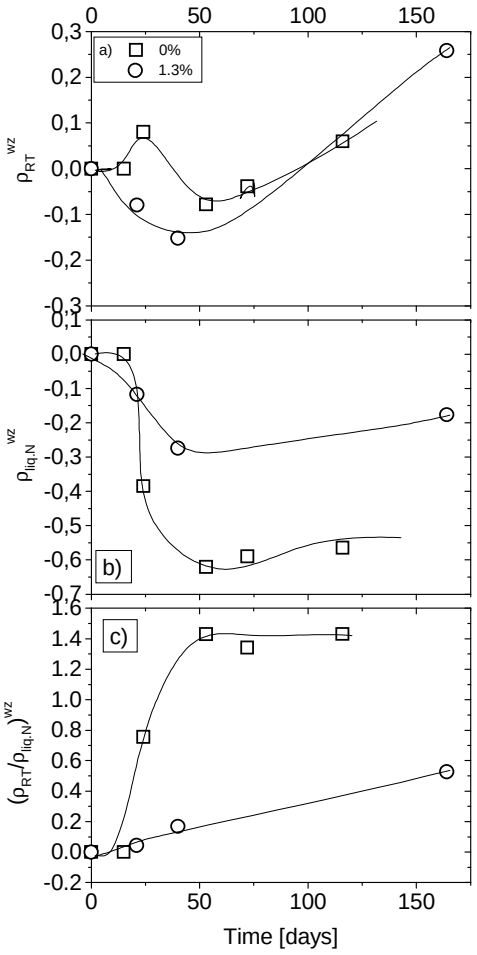

Fig. 8 – *Time variations of:*
a) the resistivity $\rho_{RT}^{rel}(\varepsilon,t)$*, b) the resistivity* $\rho_{NT}^{rel}(\varepsilon,t)$*, and*
c) the relative resistivity ratio $(\rho_{RT}/\rho_{NT})^{\mathrm{rel}}(\varepsilon,t)$ *for the samples chemically aged in the water solution of NaCl for the different degree of the plastic deformation.*

These changes depend strongly not only on the degree of the plastic deformation but also on the chemical composition of solutions. For samples plastically deformed up to 2.2% $(\rho_{RT}/\rho_{NT})^{\mathrm{rel}}(\varepsilon, t)$ was different for the different solutions used and depended on the plastic deformation degree.

3.2 X-ray study

The microstructure was studied by comparing the intensities of individual peaks for the different degrees of the plastic deformation. The results are shown in **Table 1**. In Fig. 9 the intensities of individual peaks were analysed with reference to the intensity of the (111) reflex, which is the strongest reflex in the Al standard sample – PDF 4 787 [8]. The greatest changes in the intensities are observed for the (022) reflex.

Table 1
The integral intensities of the standard and deformed samples.

hkl	(111)	(002)	(022)	(113)
Al standard (PDF 4-787)	100%	45%	20%	20%
ε [%]	Integral intensity [a.u.]			
0.0	1300	620	6800	240
0.3	290	610	11453	17
1.0	280	2280	11855	16
1.5	360	895	6890	20

Table 1 shows that the integral intensities of the material tested are different from the intensities of the Al standard. This suggests that some texture development takes place in the material tested. The intensities of the (022) reflexes increased and are the strongest in the samples measured, while in the standard samples the intensity of this reflex is only 20%. The (111) reflex is the strongest in the standard samples, but in the samples measured it is much weaker. Disproportion in the intensities of diffraction lines is attributed to the texture effect. In wires only an axial texture occurs [9].

The measurements of changes in the reflex intensities were therefore limited to the measurements on samples inclined at the reflection angles α within a

range of 90 to 30° [9] for wires positioned parallel to a diffractometer and perpendicular to an X-ray beam plane at α = 90°. The measurement results are presented in Fig. 10. For the (111) reflex the maximum of the reflex intensity occurs at α = 70° for all the samples. In the case of the (002) reflex the maximum intensity appears at α = 55°. For the (022) reflex two maximums were found; one at α =90° and other at α = 35°. By comparing our experimental data and those of the literature two directions of the texture axes: <111> and <100> were noticed. These directions are characteristic of the fcc metals [10].

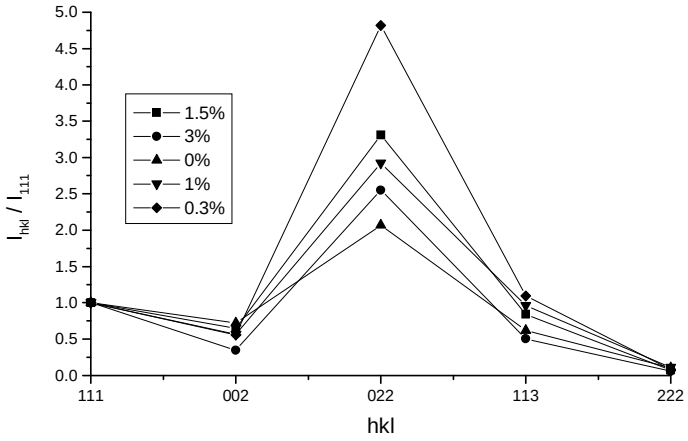

Fig. 9 – *The I_{hkl}/I_{111} relative intensity of the (111), (002), (022), and (113) reflexes for deformed samples (ε = 0.0; 0.3; 1.0; 1.5, and 3.0%).*

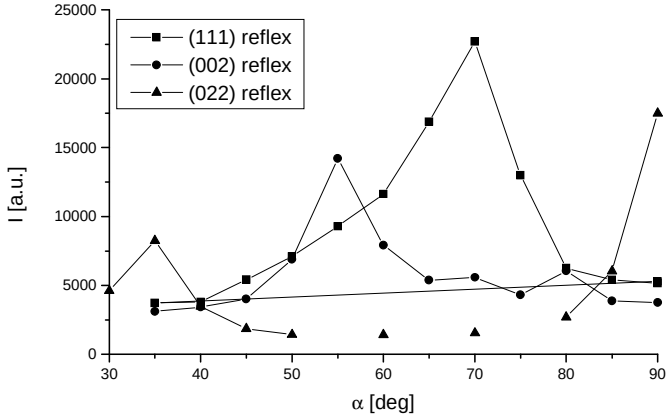

Fig. 10 – *The intensity changes of the (111), (002), and (022) reflexes for the different reflection angles α.*

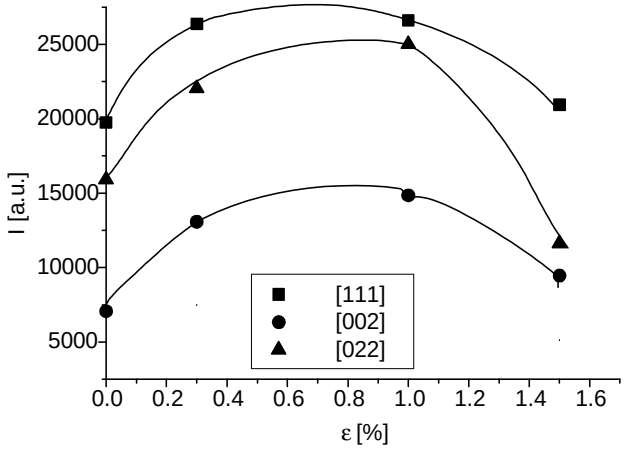

Fig. 11 – *The intensity changes of the poles versus the degree of the plastic deformation.*

The maximum intensity of the poles plotted against the degree of the plastic deformation is shown in Fig. 11. The weakest intensities occur in nondeformed samples. The greatest intensities are observed for about $\varepsilon = 1\%$. On the basis of that data it is suggested that the texture development and the degree of the plastic deformation correlate to each other.

3.3 Discussion

The initial increase in the relative resistance for the samples aged in the Na_2SO_4 water solutions, as measured at room temperature occurs only for nondeformed samples. The increase can be caused by some relaxation processes that can occur at the interface between the alloy and the passive layer [11].

The plastic deformation introduces dislocations [12, 13]. In the stress field of the dislocations the defect (vacancy) relaxation occurs. In consequence, the degree of a structure ordering increases while the resistivity decreases. Besides the dislocations prevent the passive layer damage and thus the wire resistance does not change as the Al–wire cross-sectional size does not change.

In the case of the wire samples immersed in the Na_2SO_4 water solutions the initial 20-day strong increase of $\rho_{RT}^{rel}(\varepsilon, t)$ occurs. This increase does not occur at the liquid nitrogen temperatures. It is believed that it is due to mechanical stresses at the interface between Al–alloy and its passive layer caused by rapid cooling. During the chemical ageing the region of mechanical stresses becomes

the zone of a vacancy relaxation. Therefore the quenching and the plastic deformation are similar.

In the NaCl–Na_2SO_4 solution the low degree of the plastic deformation causes the decrease in $(\rho_{RT}/\rho_{NT})^{\mathrm{rel}}(\varepsilon, t)$ while in the nondeformed samples $(\rho_{RT}/\rho_{NT})^{\mathrm{rel}}(\varepsilon, t)$ increases. The decrease in $(\rho_{RT}/\rho_{NT})^{\mathrm{rel}}(\varepsilon, t)$ in the deformed samples is attributed to the rise of a defect scattering component. The increase in the defect scattering is not observed when the plastic deformation is higher than 2%. In this case ($\varepsilon > 2\%$) the vacancy relaxation takes place near the dislocation lines.

It can therefore be said that the initial increase in a $(\rho_{RT}/\rho_{NT})^{\mathrm{rel}}(\varepsilon, t)$ value, as observed in nondeformed samples, results from the relaxation mechanism of a different character than that of the chemical relaxation of vacancies that occurs during the ion flow. This is the physical relaxation that is caused by the interaction between dislocations or between precipitates [12, 13].

The plastic deformation, excluding the Na_2SO_3–NaCl solution and $\varepsilon < 2\%$, for the long ageing time causes the $\rho_{RT}^{rel}(\varepsilon, t)$ value to decrease more rapidly than in the nondeformed samples. The initial decrease in the resistivity of the deformed wires results from the ordering of a material microstructure.

The plastic deformation less than 2% causes the increase in the $\rho_{NT}^{rel}(\varepsilon, t)$ value. It is attributed to the formation of new defects: dislocations and vacancies. The further increase in plastic deformation does not cause the $\rho_{NT}^{rel}(\varepsilon, t)$ increase despite the more and more intensive formation of dislocations within this range of the deformation.

The observed changes in the resistivities and the intensities of X-ray reflexes with the degree of the plastic deformation can be attributed to the phenomenon of the anisotropy of electrical resistivity [3]. To understand all the processes taking place during the simultaneous occurrence of the plastic deformation and the chemical ageing, and the influence of both processes on the Al–alloy resistivity, further experimental and theoretical studies are required.

4 Conclusion

The plastic deformation and chemical attack exert a significant influence on the Al-alloy resistivity. The resistivity changes can be related to the structural changes, i.e. the vacancy and dislocation formation, the vacancy relaxation or the texture effects.

It is believed that the results presented will be a certain contribution to the research upon the Al-alloy chemical ageing processes and its influence on the alloy resistivity. As supposed, the results of further research can be of great value while diagnosing the overhead lines.

7 References

[1] Report on aeolian vibration, Working Group 01 of Study Committee 22 (overhead lines), Electra 124 (1989) 40–77.

[2] Progress in non-destructive testing, ed. E.G. Stanford, J.H. Fearon, London Heywood & Company Ltd, vol. 2 (1960) 79.

[3] Y. Ueda, H. Tamura, E. Hashimoto, J. Physics: Condens. Matter, 7 (1995) 361.

[4] Su-Il Pyun, Moon-Hee Hong, Hong-Pyo Kim: Kinetics of stress corrosion crack propagation in AA 7039 using double cantilever beam specimens, Br. Corros. J., 26 (1991) 260.

[5] M.A. Lang, I. Altpeter, G. Dobman, Ein neuer Verfahrensansatz zur Fruherkennung wasserstoffinduzierter Spannungsrisskorrosion, Materials and Corrosion, 46 (1995) 422.

[6] G. Barkleit, F. Schneider, K. Mummert, Untersuchungen zum Einfluss von Sulfationen auf die chloridinduzierte lokale Korrosion am Stahl 1.4541 bei Temperaturen bis zu 280°C und gleichzeitiger Werkstofoffdehnung, Materials and Corrosion 48 (1997) 822.

[7] L.S. Zevin, G. Kimmel, Quantitative X–Ray Diffractometry, Springer–Verlag, New York, 1995.

[8] Standard References Materials (SRM), International Centre for Diffraction Data, (1995).

[9] H.P. Klug, L.E. Alexander, X–ray Diffraction Procedures for Polycrystalline and Amorphous Materials, John Wiley & Sons, New York, 1974.

[10] P. Coulomb: Les textures dans les metaux de reseau cubique, Dunod, Paris, 1972.

[11] Corrosion, ed. L.L. Shhreir: Corosion of Metals and Alloys, Vol. 1, George Newnes Ltd., London, 1969.

[12] R.W. Cahn: Physical Metallurgy, North-Holland Publishing Company, Amsterdam, 1965.

[13] Kelly, R.B. Nicholson: Strengthening Methods in Crystals, Elsevier Publishing Company Ltd., Amsterdam, 1971.